Topological insulators

Jan Masák

Abstract

This report provides a pedagogical overview of topological insulators, with a primary focus on the two seminal papers by Kane and Mele, 'Quantum Spin Hall Effect in Graphene' [1] and '$\mathbb{Z}_2$ Topological Order and the Quantum Spin Hall Effect' [2]. To give broader context and facilitate understanding also related topics are explained. First the discussion begins with the mathematical description of topological phases in band theory, introducing vector bundles and their topology. The Haldane model is then presented as a prototype for Chern insulators and as a foundation for understanding the structure of the Kane-Mele model, which in the absence of spin mixing reduces to two copies of Haldane's model. Throughout, the emphasis is on applications and interpretations relevant to the Kane-Mele works. The project was prepared as part of the seminar course 'Topics in Theoretical Physics: Topological Order in Quantum Matter' at the Faculty of Science, Leiden University, in Spring 2025.

Contents

1 Introduction

Topological insulators are materials which represent a class of insulating phases which cannot be distinguished by spontaneous symmetry breaking of local order parameters as in the usual Landau theory of phase transitions. Instead, their distinctive properties arise from the global features of their electronic structure, specifically from its topology. In any insulator, the valence bands are clearly separated from the conduction bands by an energy gap, and the collection of valence bands can be understood as forming a distinct vector bundle over the Brillouin zone (a Bloch bundle). This vector bundle can then have non-trivial topology, and that is what distinguishes a conventional (trivial) insulator from a topological insulator.

Topology classifies spaces based on equivalence classes where spaces are considered equivalent if they can be continuously transformed into each other (they are homeomorphic). Here, continuous transformations correspond to adiabatic deformations, so for example, a non-trivial insulator cannot be adiabatically transformed into a trivial one. This is at least the simplest picture. In most of this report, we actually look at the $\mathbb{Z}_2$ classification, which adopts a more fine-grained view, where one allows only symmetry-preserving deformations (equivariant homeomorphisms).

On the boundary between a non-trivial and a trivial insulator there is a phase transition (a non-adiabatic change), and as with the usual second-order phase transitions, this is associated with gapless states. Thus, topological insulators have metallic surfaces. The exotic properties of these surface states are a hallmark of topological insulators and offer the possibility for interesting applications.

The importance of topological methods in understanding new kinds of quantum order and phase transitions was recognized by the 2016 Nobel Prize in Physics awarded to Kosterlitz, Thouless, and Haldane. However, already in 1980, the integer quantum Hall effect was discovered [3], where sharply quantized Hall conductivity was observed despite the presence of impurities. Only later did the TKNN paper [4] link this conductivity to the Chern topological invariant, making it thus a topological property. The integer quantum Hall effect can thus be thought of as what is nowadays called a Chern insulator, and since the Hall conductivity σ_{xy} is directly proportional to the Chern number c_1 through the TKNN formula $\sigma_{xy} = \frac{e^2}{h} c_1$, this topological invariant becomes essentially directly experimentally observable.

Haldane's model [5] later extended these ideas to a system without net magnetic flux in graphene, realizing what is now known as the quantum anomalous Hall effect. However, Haldane's model itself does not have a natural experimental realization in any known material. This served as an inspiration for a major advance that came with the seminal work of Kane and Mele [1], who showed that strong spin-orbit coupling in graphene can lead to a new kind of insulating phase, protected by time-reversal symmetry and characterized by a $\mathbb{Z}_2$ topological invariant. Although the Kane-Mele model is not realized in graphene due to the weakness of spin-orbit coupling, similar model has been experimentally realized in other materials, most notably in HgTe quantum wells as demonstrated in [6]. In some regions this phase exhibits the so-called quantum spin Hall effect, where the spin Hall conductivity σ^s_{xy} is related to the $\mathbb{Z}_2$ index z_2 as $\sigma^s_{xy} = \frac{e}{2\pi} z_2$. This is very similar to the way the Chern number is related to the standard Hall conductivity. But as we will see, there are regions in the $\mathbb{Z}_2$ phase where the spin Hall conductivity is no longer quantized, but the edge states persist.

Since then, the study of topological phases has rapidly expanded, leading to the 'peri-

odic table' [7] classification of topological insulators and superconductors, a direct bridge between abstract mathematics and real quantum materials. It is perhaps surprising, and rather delightful, that concepts like fibre bundles, characteristic classes, and even K-theory, once thought to belong mainly to the realms of pure mathematics and theoretical fields like string theory, have found natural and concrete applications in describing electrons in solids.

From a practical point of view, topological phases may be a promising direction to explore for technological applications. Right now, there is an ongoing search for Majorana quasiparticles in engineered topological superconductors (not insulators but within the same theoretical framework), a key ingredient in proposals for topological quantum computing, which promises error protection at the hardware level. Companies such as Microsoft are actively pursuing this idea [8], although it remains an open question how close we are to realizing a practical quantum computer based on these principles. Indeed, some high-profile claims have been met with scepticism from the scientific community, but the ongoing effort shows the broad interest and potential of topological phases.

The topic of this report is based around the original works of Kane and Mele [1, 2], which laid the foundation for the study of $\mathbb{Z}_2$ topological insulators. However, the structure is closer to that of more pedagogical expositions, especially the review by Fruchart and Carpentier [9]. For an accessible introduction to the mathematical aspects, particularly in Section 2, I have also drawn from [10], which itself is based in large part on [11].

I admit that my treatment of the subject is sometimes even unnecessarily mathematical (mainly in Section 2), and the reader is encouraged to skip over technicalities, such as some formal definitions, and return to them only if needed, often, they are not essential. I also present major experimental achievements related to the topic, but do not go into much detail; these are probably somewhat under-represented compared to the literature. A very nice introduction to the subject, written from a more physics-based perspective, was also given by Kane himself [12], which I occasionally cite and consider to be perhaps the best introduction to the field.

The remainder of this report is structured as follows: first, I introduce the mathematical background needed to describe topological phases in band insulators, including vector bundles and topological invariants. Then, I discuss the key physical models in graphene. First I discuss the Haldane's model on which I illustrate the theory of Chern insulators in Section 3. In the remaining of the report I focus on the Kane-Mele model of graphene and its $\mathbb{Z}_2$ topological phase. First I introduce it and illustrate the theory on a simpler case where it reduces to two Haldane models in Section 4 and then build on this and extend it to more general setting with additional details in Section 5.

2 Topological description of band theory

In this section, I introduce some mathematical background that will be useful for the remainder of the report. The discussion goes a little beyond what is strictly necessary to understand the physics and readers should feel free to skip over technical sections or formal definitions and return to them only if needed. Rather than presenting the full mathematical framework found in most mathematical texts, I try to focus on the concepts that appear later in the discussion. I hope that offering a glimpse into the mathematical treatment of these topics will be interesting for physicists, while also helping to place the physics in a broader context and on a firmer foundation.

2.1 Vector bundles

To see how topological phases arise, it is useful to introduce a bit of the mathematical theory of vector bundles. This subsection gives a general introduction to complex vector bundles. This is sufficient for understanding Chern insulators, but we will build on it in Subsection 2.3, where we extend the ideas to treat $\mathbb{Z}_2$ insulators. The connection to physics will be discussed in the following subsection.

Let us take a topological space X (later, our Brillouin zone), which could, for example, be a torus. A complex vector bundle E over the *base space* X is essentially a topological space constructed from X by attaching to each point $x \in X$ a vector space $E_x \simeq \mathbb{C}^n$. These vector spaces E_x are called the fibres of the bundle, and can be thought of as 'living above' each point x in the base space X. This might remind one of the Cartesian product $X \times V$, and rightly so: the notion of a vector bundle generalizes this concept, and $X \times V$ can actually be thought of as a vector bundle, which we call the *trivial vector bundle*. However, just as manifolds are in general only locally flat, general vector bundles are only locally a Cartesian product. All of this is summarized in the following pseudoformal definition:

Definition (Complex vector bundle)**.** *A complex vector bundle over X is a pair (E, π) of a topological space E and a projection $\pi : E \to X$, satisfying:*

- *For every $x \in X$, the fibre $E_x := \pi^{-1}(x)$ is a finite-dimensional complex vector space.*
- *It is locally homeomorphic to $U \times \mathbb{C}^n$ for some open $U \subset X$ (i.e., locally a Cartesian product).*

The projection map π can be thought of as indicating to which point of the base space a given point of E belongs (i.e., which fibre it is part of).

We consider two complex vector bundles to have the same topology if there is an isomorphism of vector bundles between them. In that case, we say they are isomorphic as bundles and write $E \simeq F$. The definition is as follows:

Definition (Isomorphism of complex vector bundles)**.** *Let (E, π_E) and (F, π_F) be complex vector bundles over a topological space X. A homeomorphism from E to F is a continuous map $f : E \to F$ such that:*

- *$\pi_F \circ f = \pi_E$ (preserves the base points of the fibres).*
- *For all $x \in X$, the restriction $f : E_x \to F_x$ is a linear map.*

Using this, we can now see when a vector bundle is *topologically trivial*: this is when $E \simeq X \times V$. Probably the simplest intuitive example of a trivial and non-trivial bundle is that of a cylinder and a Möbius strip. To make it even more simple and relatable to the later discussion we choose the fibres to be isomorphic to vector space $\mathbb{Z}_2$ (1D vector space over the field $\mathbb{Z}_2$). Visually this gives it kind of band structure illustrated in Figure 1. We choose as the base topological space simply the circle $X = \mathbb{S}^1$. In Figure 1 one can see two vector bundles of this type: on the left there is a cylinder like vector bundle and on the right a Möbius strip like one. It turns out that the cylinder like vector bundle is topologically trivial (isomorphic to $\mathbb{S}^1 \times \mathbb{Z}_2$ as a $\mathbb{Z}_2$ bundle) and the second bundle is an example of a topologically non-trivial bundle due to its 'twist'.

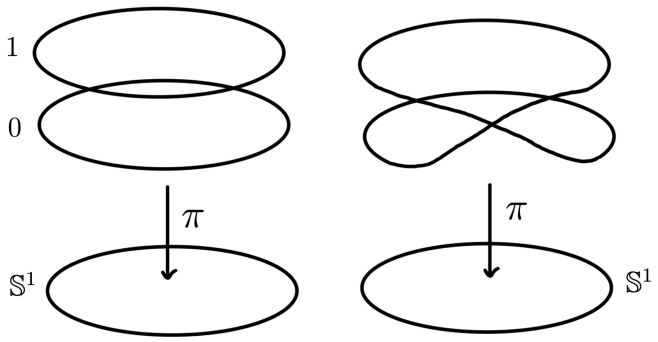

Figure 1: Depiction of two vector bundles with fibres $\mathbb{Z}_2$, base space $\mathbb{S}^1$ and projection π. In the cylinder like vector bundle on the left we can globally label the 'bands' which corresponds to a global section and the bundle is thus trivial ($\mathbb{S}^1 \times \mathbb{Z}_2$). On the other hand the Möbius like bundle on the right in topologically non-trivial as the bands can't be globally labelled.

As we will see, certain complex vector bundles, the Bloch bundles, will be natural objects to study in topological insulators, and we will be interested in those that are topologically non-trivial. At least, this is the picture for the simpler Chern insulators. The situation for $\mathbb{Z}_2$ insulators is described in Subsection 2.3.

The mathematical discipline that tries to classify vector bundles over a given space X up to isomorphism is called K-theory. The central object that one encounters, and which we will also encounter (though not use explicitly), is the K-group $K(X)$. If one considers vector bundles over the same space X, one can naturally introduce a direct sum of bundles $E \oplus F$, defined by fibres $(E \oplus F)_x = E_x \oplus F_x$. This operation is commutative, $E \oplus F \simeq F \oplus E$, and associative, $(E \oplus F) \oplus G \simeq E \oplus (F \oplus G)$ (up to isomorphism). This makes the classes of bundles into a commutative semigroup. To every commutative semigroup, there essentially corresponds a unique Abelian (commutative) group called the Grothendieck group, which is exactly our group $K(X)$. For $\mathbb{Z}_2$ insulators it is similar but slightly different, as described again in Subsection 2.3. Although it requires some mathematical technicalities to see how these K-groups translate to the invariants we encounter, it explains, for example, why the Chern's topological invariants (introduced in Subsection 3.2) of a given space form the Abelian group $\mathbb{Z}$ (the set of Chern numbers).

A useful tool for detecting whether a bundle is trivial or not is the notion of *sections*.

Definition (Section of a complex vector bundle)**.** *A section of a complex vector bundle (E, π) is any continuous map ψ from some open $U \subset X$ to E such that $\forall x \in U$: $\psi(x) \in E_x$. ψ is called global if $U = X$.*

Readers unfamiliar with sections may recognize the notion of a vector field. Indeed, the collection of all tangent spaces of a manifold forms a vector bundle, the tangent bundle, and in this case, sections and vector fields are the same thing. A global section would be an everywhere-defined vector field. Also, gauges can be understood as sections of certain bundles. The following theorem makes sections useful for our purposes:

Theorem (Sections and triviality of a complex vector bundle)**.** *A complex vector bundle is topologically trivial $\iff$ There is a set of global sections that form a basis of each fibre.*

This is equivalent to saying that if one can continuously define a frame (basis of each fibre) the vector bundle is trivial. If the fibres are 1D we need only a global nonvanishing section (gauge). This will be the case for Chern insulator and is also the case in the example of Figure 1. In this figure the choice of a global section amounts to globally labelling the bands which is similar in spirit to the case in the two valence band model of Sections 4 and 5 (the bands having there the real physical meaning of graphene energy bands). The theorem above can then be intuitively seen in Figure 1 as in the trivial bundle on the left we can globally label the bands whereas not in the non-trivial bundle on the right. However, theorem above has to be slightly modified for $\mathbb{Z}_2$ insulators which we will see in Subsection 2.3.

2.2 Bloch bundle

Having introduced the general notion of vector bundles, we now turn to the most relevant example in band theory: the *Bloch bundle*. This construction captures the geometric structure of electronic bands in crystalline solids and can be used to define some topological phases. The treatment of this subsection is based mainly on [9, 12].

Completely general classification of topological phases is a formidable task and has not yet been achieved till today [12]. However, much has been achieved with the tremendous assumptions of translational invariance and non-interacting electrons (like the Kitaev classification [7]). This is because that allows us to put to use the Bloch theorem and consider just single-particle states (many body states can be constructed from these through Slater determinant). And actually we can also consider systems that are only adiabatically connected to these assumptions since our considerations are topological.

According to Bloch's theorem, the single-particle states can be written as

$$|\psi_\alpha(\mathbf{k})\rangle = e^{i\mathbf{k}\cdot\mathbf{R}}\,|u_\alpha(\mathbf{k})\rangle\ ,$$

where $\mathbf{k}$ is a crystal momentum in the Brillouin zone, $\mathbf{R}$ is a lattice vector, and $|u_\alpha(\mathbf{k})\rangle$ is a cell-periodic function. The index α labels the bands, so that for n valence and n conduction bands it ranges from 1 to $2n$. Because of the periodicity, the Brillouin zone is topologically a torus $\mathbb{T}^2$ (throughout this report we consider only 2D systems). As already alluded to in the previous subsection Brillouin zone will play for the Bloch bundle the role of the base topological space X. For simplicity, we will refer to $|u_\alpha(\mathbf{k})\rangle$ as a *Bloch function*.

It is also useful to introduce the *Bloch Hamiltonian*

$$H(\mathbf{k}) = e^{-i\mathbf{k}\cdot\mathbf{R}} H e^{i\mathbf{k}\cdot\mathbf{R}}\,,$$

eigenvectors of which are the Bloch functions so that

$$H(\mathbf{k})\,|u_\alpha(\mathbf{k})\rangle = E_\alpha(\mathbf{k})\,|u_\alpha(\mathbf{k})\rangle\ .$$

For each $\mathbf{k}$, the set of all Bloch functions spans a Hilbert space we denote $\mathcal{H}_\mathbf{k} \simeq \mathbb{C}^{2n}$. $\mathcal{H}_\mathbf{k}$ can be then understood as a fibre over the point $\mathbf{k}$ of a complex vector bundle over the Brillouin torus $\mathbb{T}^2$. We call any such bundle a *Bloch bundle*.

The total space of the Bloch bundle of all bands is then

$$\mathcal{H} = \bigsqcup_{k\in\mathbb{T}^2} \mathcal{H}_\mathbf{k}\,.$$

It is always topologically trivial: $\mathcal{H} \simeq \mathbb{T}^2 \times \mathbb{C}^{2n}$. However, the structure becomes more interesting in the case of insulators, where there is an energy gap separating the n lowest (valence) bands from the higher (conduction) bands. The presence of this gap allows the Bloch bundle to be split into two subbundles:

$$\mathcal{H}^-_{\mathbf{k}} = \text{span}\{|u_\alpha(\mathbf{k})\rangle : E_\alpha(\mathbf{k}) < E_F\} \simeq \mathbb{C}^n \qquad \text{(valence bundle)}$$
$$\mathcal{H}^+_{\mathbf{k}} = \text{span}\{|u_\alpha(\mathbf{k})\rangle : E_\alpha(\mathbf{k}) > E_F\} \simeq \mathbb{C}^n \qquad \text{(conduction bundle)}$$

where E_F is the Fermi energy. Both the valence and conduction bundles are themselves examples of Bloch bundles, in the sense described above.

A crucial feature is that, because of the gap, the division into valence and conduction bundles is robust under adiabatic (i.e., sufficiently slow) changes in the Hamiltonian. According to the adiabatic theorem, the energy gap sets a scale for how slowly these changes must occur in order for the system to remain in its instantaneous ground state throughout the deformation. In this way, the physical notion of adiabatic continuity corresponds directly to the mathematical notion of continuous deformation of the bundle: as long as the gap remains open, the topology of the valence bundle cannot change.

It is important to note that, although the Bloch bundle of all bands is always topologically trivial, the separation into subbundles can cause the valence bundle to obtain non-trivial topology. One can detect this for example by non-trivial topological invariants such as the Chern number (Subsection 3.2) and the $\mathbb{Z}_2$ invariant (Subsections 4.2 and 5.2).

Moreover, since the band structure is fully determined by the Bloch Hamiltonian, classifying possible valence bundles is therefore equivalent to classifying the possible gapped Bloch Hamiltonians (up to adiabatic deformation) compatible with a given set of symmetries. This point of view is at the heart of the modern classification schemes, such as the Kitaev periodic table [7], which systematically organizes free-fermion systems by their symmetry class and the resulting topological types of their valence bundles. Underlying this classification is the algebraic structure of symmetry constraints, which is often described using representations of Clifford algebras which we will encounter in our discussion of both Chern (in Subsection 3.1) and $\mathbb{Z}_2$ topological insulators (in Subsection 4.1).

2.3 Quaternionic vector bundles

In the study of $\mathbb{Z}_2$ insulators, we encounter time-reversal symmetry. In the case relevant here, the time-reversal operator Θ is anti-linear and satisfies $\Theta^2 = -I$ (anti-involutive).

Having such an operator on a complex vector space of dimension $2n$ is essentially equivalent to having a quaternionic 'vector space' of dimension n (or, more precisely, a module, since the quaternions $\mathbb{H}$ are not a field due to their non-commutativity). This correspondence arises because, in addition to complex scalar multiplication (by i), we can interpret the action of Θ as multiplication by a second imaginary unit j, with $k = ij$, satisfying the quaternion relations $i^2 = j^2 = k^2 = ijk = -1$.

Now that we understand the action of time-reversal symmetry on a vector space, we can generalize it to introduce the notion of a quaternionic vector bundle. As we will see in Sections 4 and 5, this is motivated by the Bloch bundle description of $\mathbb{Z}_2$ topological insulators. The linear map Θ in there will then exactly correspond to what we will call Θ in the following definitions, and the map θ will be defined as $\theta(\mathbf{k}) = -\mathbf{k}$.

Definition (Quaternionic vector bundle)**.** *A quaternionic vector bundle is a complex vector bundle (E, π) over a topological space X equipped with:*

- *An involutive homeomorphism θ on X.*
- *An anti-linear homeomorphism Θ such that $\Theta : E_x \to E_{\theta(x)}$ for each $x \in X$ and $\Theta^2 = -I$ on each fibre.*

In this definition one can notice that in general the fibres of a quaternionic vector bundle in general do not have a natural structure of a quaternionic vector space as discussed at the beginning of this section. However, we have this structure for fibres above points that are fixed points of the map θ. These are important points which play a crucial role for example in the calculation of the $\mathbb{Z}_2$ invariant in Subsection 5.2 where we call them time reversal invariant momenta (TRIM). Indeed, also one possibility how to approach the classification of quaternionic vector bundles is to in some sense focus on these points as is discussed in [10].

In later discussion the operator Θ will act on Bloch functions as $\Theta\,|u_\alpha(\mathbf{k})\rangle = |u_\beta(-\mathbf{k})\rangle$. This relation can also be interpreted as saying that bands α and β form a so-called Kramers pair. We can define this important notion also within the general mathematical theory as follows.

Definition (Kramers pairs)**.** *Let us have a quaternionic vector bundle (E, π, Θ) over (X, θ) with two sections $\psi : U \to E$ and $\phi : \theta(U) \to E$. We say that ψ and ϕ form a Kramers pair if $\Theta \circ \psi = \phi \circ \theta$. A Kramers pair is called global if $U = X$.*

We also need a new notion of which bundles we consider topologically equivalent (isomorphic). For $\mathbb{Z}_2$ insulators, one should use the following definition:

Definition (Isomorphism of quaternionic vector bundles)**.**
Let (E, π_E, Θ_E) and (F, π_F, Θ_F) be quaternionic vector bundles over (X, θ). An isomorphism of complex vector bundles $f : E \to F$ is also an isomorphism of quaternionic vector bundles if $\Theta_F \circ f = f \circ \Theta_E$.

Intuitively, this says that not only do the bundles have to be isomorphic as complex vector bundles (as defined in Subsection 2.1), but the isomorphism must also respect time-reversal symmetry. Topological triviality is then defined as before, but with this new definition of isomorphism. Since our notion of topological equivalence is now stronger, bundles that might have been trivial as complex vector bundles can be non-trivial as quaternionic vector bundles. Thus, as we will see, even insulators that would be considered trivial as Chern insulators can be non-trivial as $\mathbb{Z}_2$ insulators.

Exactly as in the case of complex vector bundles, one can define a K-group for quaternionic vector bundles, $KQ(X)$, but now using the new definition of isomorphism [10]. This theory was first introduced, supposedly under the name symplectic K-theory, in [13]. It again holds that $KQ(X)$ is always Abelian, which explains the appearance of the Abelian group $\mathbb{Z}_2$ in $\mathbb{Z}_2$ insulators.

In Subsection 2.1, we had the theorem 'Sections and triviality of a complex vector bundle', which can be used as an alternative tool (to topological invariants) to search for non-trivial bundles/insulators. We now introduce the equivalent theorem for quaternionic vector bundles, which will be useful in Subsection 5.2 for understanding the calculation of the $\mathbb{Z}_2$ invariant.

Theorem (Sections and triviality of a quaternionic vector bundle)**.** *A quaternionic vector bundle is topologically trivial $\iff$ There is a set of global Kramers pairs that form a basis of each fibre.*

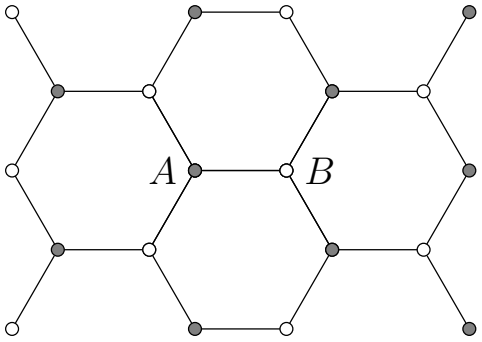

Figure 2: Section of the hexagonal (honeycomb) lattice of graphene with the two triangular Bravais sublattices A (grey sites) and B (white sites).

3 Chern insulators in graphene

Having introduced the general mathematical theory in the previous section we now put it to use on our first example of topological insulator. In this section we deal with a so called Chern insulators which are theoretically a little easier to deal with. One famous example which can be understood as a Chern topological insulator is the Integer Quantum Hall effect which requires external magnetic field but in this section we study instead a model on the graphene lattice introduced by Haldane [5] which requires no overall magnetic field and exhibits thus so-called Anomalous Quantum Hall effect. Unfortunately this model is not experimentally realized in any real material but serves as a useful tool for understanding the more experimentally relevant Kane-Mele model of graphene which we encounter in later sections and is our main focus in this report. Actually in the simpler setting of Kane-Mele model in the next section Kane-Mele model reduces just to two Haldane models.

3.1 Introduction to Haldane's model

As already alluded to, the arena of this section is going to be graphene. Graphene has a hexagonal lattice which is crucially not a Bravais lattice but consists of two triangular Bravais sublattices, as shown in Figure 2.

We can write Bloch functions on the graphene lattice with the sublattice degree of freedom as $|u(\mathbf{k})\rangle = (u_A(\mathbf{k}), u_B(\mathbf{k}))$, which live at each momentum in Hilbert spaces $\mathcal{H}_\mathbf{k} \simeq \mathbb{C}^2$, meaning that our Hamiltonian must be a 2×2 Hermitian matrix. Any such matrix can be written in terms of the Pauli matrices $\vec{\sigma}$ and four momentum-dependent real coefficients $h_0(\mathbf{k})$ and $\vec{h}(\mathbf{k})$ as

$$H_H(\mathbf{k}) = h_0(\mathbf{k})I + \vec{h}(\mathbf{k}) \cdot \vec{\sigma}\,. \tag{1}$$

This form is handy, for example, for discussion of the symmetries. You may also know that the identity with the Pauli matrices form the Clifford algebra $\mathcal{C}l(2)$ as $\{\sigma^i, \sigma^j\} = 2\delta^{ij}$; we will encounter a representation of the Clifford algebra $\mathcal{C}l(4)$ in the next section. As mentioned in Subsection 2.2, Clifford algebras have been used by Kitaev in his classification of topological phases [7]. The Hamiltonian (1) has then eigenstates

$$H_H(\mathbf{k})\,|u_\pm(\mathbf{k})\rangle = E_\pm(\mathbf{k})\,|u_\pm(\mathbf{k})\rangle \qquad E_\pm(\mathbf{k}) = h_0(\mathbf{k}) \pm h(\mathbf{k})\,, \tag{2}$$

where, as always, $h(\mathbf{k}) = |\vec{h}(\mathbf{k})|$, and the gap is thus

$$\Delta(\mathbf{k}) = E_+(\mathbf{k}) - E_-(\mathbf{k}) = 2h(\mathbf{k})\,. \tag{3}$$

Two symmetries that are going to accompany us throughout this report are the *time-reversal symmetry* Θ (TR) and the *inversion symmetry* $\mathcal{I}$ (TR will be much more important). In this system, where we have only the sublattice degree of freedom, TR physically only reverses the momenta $\mathbf{k} \leftrightarrow -\mathbf{k}$, which translates into it being an anti-unitary operator represented in this case simply as $\Theta = \mathcal{K}$ ($\mathcal{K}$ being the complex conjugation operator). Inversion symmetry physically switches the two sublattices $A \leftrightarrow B$, so $\mathcal{I}\,|u(\mathbf{k})\rangle = (u_B(\mathbf{k}), u_A(\mathbf{k})) \implies \mathcal{I} = \sigma_x$.

A unitary transformation is a symmetry of a Hamiltonian if it commutes with it. So our system has inversion symmetry if $[\mathcal{I}, H] = 0$, and TR symmetry if $[\Theta, H] = 0$. This translates into the following conditions on the Bloch Hamiltonian:

$$\mathcal{I}H(\mathbf{k})\mathcal{I}^{-1} = H(-\mathbf{k})\,, \tag{4}$$

$$\Theta H(\mathbf{k})\Theta^{-1} = H(-\mathbf{k})\,. \tag{5}$$

Another symmetry that comes into play here is the C_3 symmetry of the lattice, which comes from the sites of the lattice being invariant under rotation of the connecting 'bonds' by 120° (see Figure 2). This symmetry then dictates that $h_x(\mathbf{k})$ and $h_y(\mathbf{k})$ vanish at the K points ($\pm\mathbf{K}$), which are the famous points in the Brillouin zone where the conduction and valence bands touch in standard graphene. Substituting this into (3) we have $\Delta(\pm\mathbf{K}) = 2|h_z(\pm\mathbf{K})|$. Normally the gap vanishes because (4) dictates that $h_z(\mathbf{k})$ is everywhere an odd function (i.e., $h_z(\mathbf{k}) = -h_z(-\mathbf{k})$) and (5) that it is everywhere even (i.e., $h_z(\mathbf{k}) = h_z(-\mathbf{k})$), which forces h_z to vanish when these symmetries are present. Thus, with these symmetries, $\Delta(\pm\mathbf{K}) = 0$ and we do not have an insulator. As we are interested in insulators (specifically, ones with non-trivial topology), we need to break at least one of these symmetries. We cannot, of course, break the C_3 symmetry as it is a symmetry of the lattice, but we can break TR and inversion symmetry, and in Subsection 3.3 we will see breaking of both. However, we will also learn in the next subsection that the topology would always be trivial in the presence of time-reversal symmetry, so it needs to be broken for us to have a topological insulator.

3.2 Chern's topological invariant

Topology is used here in a somewhat flexible sense, as the reader may recall from Section 2: Chern insulators and $\mathbb{Z}_2$ insulators each have their own notion of what it means for two systems to be 'topologically equivalent'. In this section, we focus on the standard setting introduced in Subsection 2.1, where topology refers to the classification of complex vector bundles.

A topological invariant is a quantity that remains unchanged under continuous deformations that preserve the topology of the system. Thus, if two systems have different topological invariants, they must also differ topologically, though the converse does not necessarily hold: two topologically distinct objects may share the same value of a given invariant. An important consequence for us is that if any topological invariant of a vector bundle differs from that of the trivial bundle, the bundle must be topologically non-trivial. While mathematicians consider invariants in form of different mathematical objects, we will focus here on numerical invariants. Notably, these numbers can often be related directly to physical observables, such as the quantized Hall conductivities.

A key mathematical result, Chern-Weil theory, provides a powerful link between geometry and topology. It states that, whenever a vector bundle is associated to a gauge theory (in mathematical language, our vector bundle is associated bundle to some principal

fibre bundle), one can construct topological invariants from the corresponding curvature form. A celebrated special case that provides some intuition for this is the Gauss-Bonnet theorem, where the relevant bundle is the tangent bundle of a Riemannian manifold, and the associated curvature is just the Riemann curvature. The Gauss-Bonnet theorem can be then expressed as

$$\chi(X) = \int_X \mathrm{Pf}\, R,$$

where $\chi(X)$ is the Euler characteristic of X[1] and R is the Riemann curvature two-form (For two-dimensional manifolds, $\mathrm{Pf}\, R$ simply gives the Gaussian curvature.).

Remember that in the study of topological insulators we are concerned with the topology of the valence Bloch bundle (see Subsection 2.2) which is a complex vector bundle we will call E over the Brillouin zone $\mathbb{T}^2$. Natural gauge theory that we have here is gauge theory coming from the fact that the phase of a single particle wave function is not observable-a $U(1)$ gauge theory. If we choose a connection one-form A we have then corresponding curvature two-form $F = dA$. Notice here that because the connection is not unique, curvature is also not unique. But of course topological invariants will be independent of this choice, so we can choose any connection. In condensed matter physics one uses for our purposes the so-called Berry connection. All results which we use in our work (these are mainly [4, 5]) were calculated using this connection. Use of this connection assumes that the Bloch Hamiltonian $H(\mathbf{k})$ varies adiabatically with $\mathbf{k}$ which is however also what we needed to define the valence Bloch bundle, so it will always be the case. For a single valence band we are concerned with here, the Berry connection is given by

$$A = i \langle du_- | u_- \rangle := i \langle u_-(\mathbf{k}) | \, \partial_i \, | u_-(\mathbf{k}) \rangle \, dk^i, \tag{6}$$

where we used the notation of previous section.

For our specific case the Chern-Weil theory provides us with the following topological invariant of our bundle E:

$$c_1(E) = \frac{1}{2\pi} \int_{\mathbb{T}^2} F\,, \tag{7}$$

which is called the *Chern number*, and it can take only integer values ($c_1(E) \in \mathbb{Z}$). The celebrated TKNN formula [4]

$$\sigma_{xy} = \frac{e^2}{h} c_1(E) \tag{8}$$

relates the Chern number to the Hall conductivity σ_{xy} thus making the Chern's topological invariant directly observable. It also implies that the Hall conductivity is quantized which can be also used to explain the Integer Quantum Hall effect.

Let us now see what happens in the presence of time reversal (TR) symmetry. Using the definition (6) one can see that if the Bloch Hamiltonian is TR symmetric $A(-k) = -A(k)$ or in other words the Berry connection is odd under time reversal. This can be written in the more abstract mathematical language of Subsection 2.3 as $\theta^* A = -A$ with $\theta(\mathbf{k}) = -\mathbf{k}$. Using $\theta(\mathbb{T}^2) = \mathbb{T}^2$ this than implies that the Chern number must vanish when TR is present as

$$c_1(E) = \frac{1}{2\pi} \int_{\theta(\mathbb{T}^2)} F = \frac{1}{2\pi} \int_{\mathbb{T}^2} \theta^* F = \frac{1}{2\pi} \int_{\mathbb{T}^2} d(\theta^* A) = -\frac{1}{2\pi} \int_{\mathbb{T}^2} dA = -c_1(E)\,.$$

[1]Here the Euler characteristic depends only on the base space X and not on the whole vector bundle as will be later the case with Chern numbers since we are dealing with the tangent bundle which is uniquely determined by the base manifold.

And actually it turns out that the valence Bloch bundle is always topologically trivial in the sense of Subsection 2.1 in a TR invariant system [9]. One can only have non-trivial topology in the sense of Subsection 2.3. As in the next subsection we are interested in the first sense of non-trivial topology, we must break time reversal symmetry to have non-trivial topology.

In our model, we consider just a single-band valence Bloch bundle. As Bloch functions must be normalized, a continuous choice of Bloch function (which, in the language of Subsection 2.1, is a section) is equivalent to choosing a gauge. Notice that when we can choose a global gauge, and thus also have a global section, we have, by Stokes theorem,

$$c_1(E) = \frac{1}{2\pi}\int_{\mathbb{T}^2} dA = \frac{1}{2\pi}\int_{\partial\mathbb{T}^2} A = 0\,,$$

since $\partial\mathbb{T}^2 = \emptyset$. This is exactly in accordance with the theorem at the end of Subsection 2.1, since as we have just one band, a single global section is sufficient to obtain a basis of $\mathcal{H}_{\mathbf{k}}$ at every $\mathbf{k}$.

If we do not have a global gauge, we cannot do this because A, and thus F, are not globally defined. However, to get closer to the general expression for the $\mathbb{Z}_2$ invariant we will encounter in Subsection 5.2, we now consider a more general case having $\mathbb{T}^2$ covered by two open sets U and U', where we can choose gauges ($\mathbb{T}^2 = U \cup U'$). For our purposes, the intersection can be taken to be a contour, $\partial U = U \cap U' = -\partial U'$ (where $-$ here denotes the opposite orientation). One also has a gauge transformation $g : U \cap U' \to U(1)$, $g(\mathbf{k}) = e^{i\phi(\mathbf{k})}$, defined through $|u'_-(\mathbf{k})\rangle = g(\mathbf{k})\,|u_-(\mathbf{k})\rangle$ (equivalent to $g(\mathbf{k}) = \langle u_-(\mathbf{k})|u'_-(\mathbf{k})\rangle$). Let A be our connection in the gauge on U and A' on U'. Using Stokes theorem we have

$$c_1(E) = \frac{1}{2\pi}\int_{\mathbb{T}^2} F = \frac{1}{2\pi}\left(\int_U dA + \int_{U'} dA'\right) = \frac{1}{2\pi}\left(\int_{\partial U} A + \int_{\partial U'} A'\right) = \frac{1}{2\pi}\int_{\partial U}(A - A')\,.$$

We can now use the gauge transformation rule for the connection

$$A = g^{-1}A'g - ig^{-1}dg = A' + d\phi\,,$$

to rewrite this as a contour integral over the boundary of the region U:

$$c_1(E) = \frac{1}{2\pi}\oint_{\partial U} d\phi = \frac{1}{2\pi i}\oint_{\partial U} d\log g\,. \tag{9}$$

In other words, we see that in the case where we can cover the space by two gauges, the Chern number is given by the winding number of the transition function. The reader should then compare this to the expression we get in Subsection 5.2.

3.3 Anomalous Quantum Hall effect

Having introduced the general setting of Haldane's model in the Subsection 3.1 and equipped with the relevant topological weaponry from previous subsection we can have a closer look on the model and discuss its Chern number for different parameters which will give us a topological phase diagram.

Specifying a model can be thought of as choosing a specific form of the functions $h_i(\mathbf{k})$ for a Hamiltonian of the form (1). As Haldane's model is a model of graphene, we want to respect the symmetries of the lattice and, as discussed throughout this section, if we wish

to obtain a topological insulator, we must break time-reversal symmetry. This can be achieved without net magnetic flux by introducing local fluxes, as illustrated in Figure 3. This breaks time-reversal symmetry and causes the hopping parameters t_{ij} (hopping from site i to site j) to acquire an Aharonov-Bohm phase through the Peierls substitution [9]:

$$t_{ij} \to t_{ij} \exp\left(-i\frac{e}{\hbar}\int_{\gamma_{ij}} A_{\text{em}}\right) ,$$

where A_{em} is the electromagnetic vector potential and γ_{ij} is the hopping trajectory from site i to site j. In the following, we consider nearest-neighbour interactions (between the two sublattices A and B) with coupling t and second-nearest-neighbour interactions (between sites of the same sublattice) with t_2. Fluxes as in Figure 3 then translate into nearest-neighbour interactions accumulating no overall phase (Peierls substitution $t \to t$), but a phase is accumulated in the second-nearest-neighbour interactions (Peierls substitution $t_2 \to t_2 e^{\phi}$).

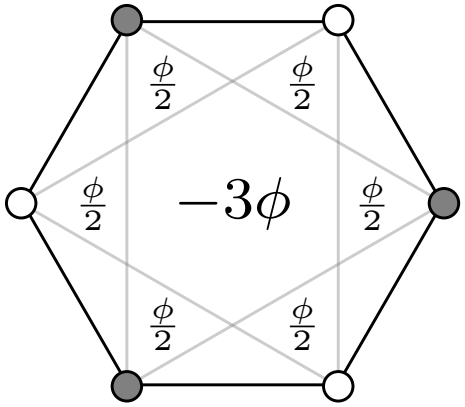

Figure 3: Scheme for magnetic flux through one hexagonal tile of the graphene lattice. As in Figure 2 sites of sublattice A are in grey and of sublattice B in white.

In general, Haldane's model can also include a staggered potential with coupling λ_v, which assigns an on-site energy λ_v to all lattice sites of type A and energy $-\lambda_v$ to all sites of type B. This manifestly breaks inversion symmetry.

All of this translates into the following parameters of the Bloch Hamiltonian (1):

$$\begin{aligned} h_0 &= 2t_2 \cos\phi(\cos(2x) + 2\cos x \cos y) , & h_y &= 2t \cos x \sin y , \\ h_x &= t(1 + 2\cos x \cos y) , & h_z &= \lambda_v - 2t_2 \sin\phi(\sin(2x) - 2\sin x \cos y) , \end{aligned} \tag{10}$$

where we use the notation of [2], in which, if $\mathbf{k} = (k_x, k_y)$, then $x := \frac{k_x a}{2}$ and $y := \frac{\sqrt{3}}{2} k_y a$, with a being the Bravais lattice constant.

Using, for example, the formula (7) with (6) or (9), one can find[2] the Chern number to be given by the expression:

$$c_1 = \frac{1}{2}\left[\text{sgn}(\Delta(\mathbf{K})) - \text{sgn}(\Delta(-\mathbf{K}))\right] , , \tag{11}$$

with the coordinates of the K points being $\pm\mathbf{K} = \left(\pm\frac{4\pi}{3a}, 0\right)$. As discussed at the end of Subsection 3.1, the gap (3) reduces to $\Delta(\pm\mathbf{K}) = 2h_z(\pm\mathbf{K}) = 2\left(\lambda_v \pm 3\sqrt{3}t_2 \sin\phi\right)$ at the

[2]The curious reader can find a derivation of this result, which is certainly interesting, for example in [9].

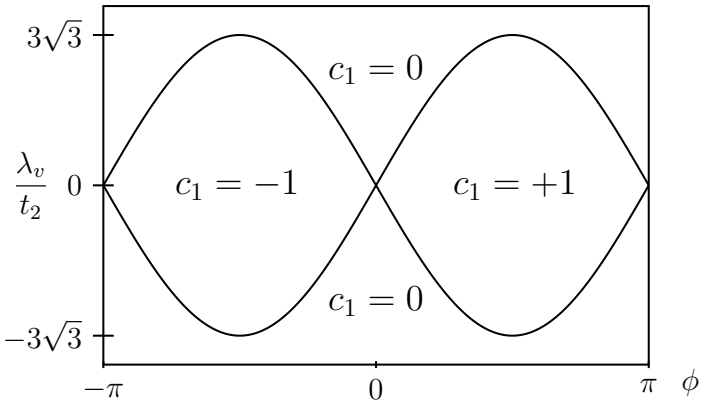

Figure 4: Topological phase diagram of the Haldane's model where the topological phases are indexed by the Chern number c_1. $c_1 = \pm 1$ corresponds to topologically non-trivial insulator and $c_1 = 0$ to a trivial insulator. This diagram can be obtained for example based on the formula (11). As ϕ is a phase $\phi = -\pi$ and $\phi = \pi$ should be identified (the space of parameters is an infinite cylinder).

K points, which is enforced by the lattice symmetry. Thus, we see that the gap vanishes at $|\lambda_v| = 3\sqrt{3}|t_2 \sin\phi|$, which gives us a line where one would expect a phase transition to occur. Indeed, based on (11), one can construct the phase diagram in Figure 4.

One can thus notice that everything that really matters for the topology happens around the K points. It is therefore of interest to expand our Bloch Hamiltonian (1) $H_H(\mathbf{k})$ around these points. Defining $\mathbf{k} = \pm\mathbf{K} + \mathbf{q}$ and linearizing in $\mathbf{q}$ (assuming $q \ll K \sim \frac{1}{a}$), one obtains:

$$H_H^{\text{eff}}(\mathbf{q}) = E_F + \hbar v_F(\mp q_x \sigma^x + q_y \sigma^y) + \Delta_H \sigma^z \,, \tag{12}$$

with $v_F = \frac{\sqrt{3}}{2}\frac{at}{\hbar}$, $\Delta_H = \lambda_v \pm 3\sqrt{3}t_2 \sin\phi$, and $E_F = -3t_2 \cos\phi$. For the energies one finds $E_{\text{eff}}^{\pm} = E_F \pm \sqrt{(\hbar v_F q)^2 + \Delta_H^2}$, and we see that indeed the gap is $\Delta(\pm\mathbf{K}) = 2|\Delta_H|$.

3.4 Chiral edges states

Essential property of topological insulators is the presence of metallic edge states at the boundaries. Let us now illustrate their presence in Haldane's model following [9].

For example, from the formula (11) it is clear that at the transition from a trivial to a non-trivial insulator there is a gap inversion at one of the K points, and right at the boundary the gap vanishes. Let us, for concreteness, consider the case when the gap reverses at the point $-K$, so that we have from (12) the effective Hamiltonian

$$H = H_H^{\text{eff}} - E_F = \hbar v_F \, \mathbf{q} \cdot \boldsymbol{\sigma} + \Delta_H \sigma^z \qquad \text{with} \qquad \Delta_H = \lambda_v - 3\sqrt{3}t_2 \sin\phi \,. \tag{13}$$

We also specifically choose the coordinate y so that $y = 0$ at the boundary, $c_1 = 1, \Delta_H(y) < 0$ for $y < 0$ (non-trivial topology) and $c_1 = 0, \Delta_H(y) > 0$ for $y > 0$.

As the mass depends on position, we must go over to the position space representation where $\mathbf{q} \to -i\nabla_{\mathbf{x}}$. We would like to solve the eigenvalue problem

$$H\psi_{\mathbf{q}}(\mathbf{x}) = \begin{pmatrix} \Delta_H(y) & -i\partial_x - \partial_y \\ -i\partial_x + \partial_y & -\Delta_H(y) \end{pmatrix} \psi_{\mathbf{q}}(\mathbf{x}) = E(\mathbf{q})\, \psi_{\mathbf{q}}(\mathbf{x}) \tag{14}$$

To separate variables, we go over to the Hadamard basis with

$$U = \frac{1}{\sqrt{2}} \begin{pmatrix} 1 & 1 \\ 1 & -1 \end{pmatrix} .$$

This is then readily solved (left as an exercise to the reader) to obtain $U\psi_{\mathbf{q}}(\mathbf{x})$. Along the way, one has to make a few choices for the solution to be integrable, and with our choices regarding the function $\Delta_H(y)$, one obtains the set of eigenstates

$$\psi_{\mathbf{q}}(\mathbf{x}) \propto e^{iq_x x} \exp\left(-\int_0^y \Delta_H(y')\,dy\right)\begin{pmatrix}0\\1\end{pmatrix}. \tag{15}$$

Actually, we could have guessed the factor $e^{iq_x x}$ since we have translational symmetry in that direction. These states have the linear dispersion $E(\mathbf{q}) = \hbar v_F\, q_x$ and are thus gapless. We also obtain group velocity $\mathbf{v}_g = \nabla_{\mathbf{q}} E(\mathbf{q}) = (v_F,\, 0)$ in the positive x direction along the boundary, and thus such states are only right-moving. Because of this directionality locking, we call such states *chiral*. Were we to have a boundary with $c_1 = -1$ instead of $c_1 = 1$, the chirality would be reversed. Also, given that $\Delta_H(y)$ changes sign at $y = 0$, it follows from (15) that $\psi_{\mathbf{q}}$ will be localized around the boundary at $y = 0$. So, all in all, we have established the presence of gapless chiral edge states.

Probably the most significant reason why the edge states are of such interest is that they are insensitive to disorder. This is because there are no states available for elastic backscattering. This, in fact, underlies the perfectly quantized electronic transport of the quantum Hall effect.

4 Quantum Spin Hall effect in graphene

In this section I first introduce the general setting of the Kane-Mele model of graphene in Subsection 4.1. The subject of Subsection 4.2 is a simplification of the model where we do not allow for spin mixing; specifically, we set the Rashba term, which will be introduced later, to zero ($\lambda_R = 0$). This assumption makes the analysis much easier, as it allows us to treat the Kane-Mele model as two separate Haldane models. Importantly, in this case the spin Hall conductance is quantized, and we can properly speak of the Quantum Spin Hall effect. Edge states are present both in this simplified model and in the full Kane-Mele model, which will be discussed in the next section. However, we will leave the discussion of edge states for later. As we will see, the presence of edge states in both the simplified and the full model is a sign that both settings ($\lambda_R = 0$ and $\lambda_R \neq 0$) can realize a non-trivial $\mathbb{Z}_2$ topological phase.

4.1 Introduction to Kane-Mele model

In the Kane-Mele model of graphene, one adds a spin degree of freedom to the sublattice degree of freedom in the description. Whereas before we had, at every momentum, the Hilbert space $\mathcal{H}_{\mathbf{k}} \simeq \mathbb{C}^2$ (in the language of Subsection 2.2 we considered $n = 1$), schematically representing the sublattice degrees of freedom and with basis of the form (A, B), now we have Hilbert spaces $\mathcal{H}_{\mathbf{k}} \simeq \mathbb{C}^4$ (in Subsection 2.2 corresponding to $n = 2$) with basis of the form $(\uparrow, \downarrow) \otimes (A, B)$.

As in Subsection 3.1, every 4×4 Bloch Hamiltonian can be written in terms of a representation of the corresponding Clifford algebra $\mathcal{C}l(4)$. That is, in terms of the identity, five Dirac matrices Γ^a, and their ten commutators Γ^{ab}:

$$\Gamma^{(1,2,3,4,5)} :=, (I \otimes \sigma^x, I \otimes \sigma^z, \sigma^x \otimes \sigma^y, \sigma^y \otimes \sigma^y, \sigma^z \otimes \sigma^y)\,,$$
$$\Gamma^{ab} := \frac{1}{2i}[\Gamma^a,\, \Gamma^b]\,, \quad \{\Gamma^a,\, \Gamma^b\} = 2\delta^{ab}\,.$$

This means that our Bloch Hamiltonian can be characterized by sixteen real coefficient functions $d_0(\mathbf{k})$, $d_a(\mathbf{k})$ and $d_{ab}(\mathbf{k})$ as

$$H_{KM}(\mathbf{k}) = d_0(\mathbf{k})I + \sum_{a=1}^{5} d_a(\mathbf{k})\Gamma^a + \sum_{a<b} d_{ab}(\mathbf{k})\Gamma^{ab}\,.$$

This representation is particularly useful when discussing the symmetries. As discussed in Subsection 2.2, we take the two bands below the Fermi level, $|u_1(\mathbf{k})\rangle$ and $|u_2(\mathbf{k})\rangle$, to form our valence band Bloch bundle.

So let us now delve into some symmetry considerations. The most important symmetry that will always be present is time-reversal (TR) symmetry. This is in stark contrast to the Haldane model considered in the previous section, as we have seen that to have a non-trivial topological insulator the TR symmetry had to be broken. Let us represent TR by the operator Θ. We want the operator to act on the spin degree of freedom as $\Theta\,|\uparrow\rangle = -\,|\downarrow\rangle$ and $\Theta\,|\downarrow\rangle = |\uparrow\rangle$, and to act trivially on the sublattice degrees of freedom. These requirements specify it as $\Theta = i\sigma^y \otimes I\,\mathcal{K}$. From this we also see that $\Theta^2 = -I$. Time-reversal symmetry also provides us with Kramers theorem, which is essential for our discussion and can be formulated for our purposes as:

Theorem (Kramers theorem)**.** *For a TR-invariant system of one electron, all energies are at least doubly degenerate. If $|\psi\rangle$ is an eigenstate of the Hamiltonian, then $\Theta\,|\psi\rangle$ is an orthogonal (since $\Theta^2 = -I$) eigenstate with the same energy eigenvalue.*

As TR reverses the momenta, the action of the TR operator on Bloch functions is $\Theta\,|u_1(\mathbf{k})\rangle = |u_2(-\mathbf{k})\rangle$, and we say that $|u_1(\mathbf{k})\rangle$ and $|u_2(\mathbf{k})\rangle$ form a Kramers pair.[3] By Kramers theorem, we then have $E_1(\mathbf{k}) = E_2(-\mathbf{k})$ and $\langle u_1(\mathbf{k})|u_2(-\mathbf{k})\rangle = 0$.[4] The presence of TR symmetry also imposes restrictions on the form of the d's. The condition of TR invariance can again be formalized as (5). This then means that $\Theta\Gamma^a\Theta^{-1} = \Gamma^a$ implies that all $d_a(\mathbf{k})$ are even functions of $\mathbf{k}$, and $\Theta\Gamma^{ab}\Theta^{-1} = -\Gamma^{ab}$ implies that d_{ab} must be odd functions.

Another important concept coming from TR symmetry are momenta for which $\mathbf{k} = -\mathbf{k}+\mathbf{G}$ for some reciprocal lattice vector $\mathbf{G}$. As the effect of TR is to reverse the momenta such momenta will be referred to as TR invariant momenta or TRIM for short. There are many interesting things happening at these point in the Brillouin zone but one thing we can immediately notice from the Kramers theorem is that at these points the Kramers partners are in the same fibre and as they are two orthonormal vectors in 2D vector space they form an orthogonal basis of this fibre. This among other means that the spectrum is at that point degenerate since Kramers partners must have according to Kramers theorem the same energy eigenvalue.

Another symmetry, also discussed in Subsection 3.1, is the inversion symmetry that switches the two sublattices. This symmetry is not as important here as TR symmetry, and it will not always be present in our model, but it is still worth discussing. We saw that, on the sublattice degrees of freedom, it can be represented in our basis by σ^x. On the spin degrees of freedom, it acts trivially, so on the full space it can be represented as

[3] All of this is defined in more mathematical terms in Subsection 2.3.

[4] Such considerations go a little against the mathematical spirit discussed in Subsection 2.3, as we are taking the inner product of vectors that are at different fibres of the valence Bloch bundle, which implicitly assumes some structure that relates these fibres. Here, it makes sense, among other reasons, because the valence bundle is embedded in the Bloch bundle of all bands, which is always trivial.

Symmetry (physical meaning)	t	λ_{SO}	λ_R	λ_v
$U(2)$ $U(1)$ (charge conservation)	✓	✓	✓	✓
$U(2)$ $SU(2)$ (spin conservation)	✓	$\times$ to $U(1)$ (only S_z)	$\times$	✓
z-Mirror (protects S_z conservation)	✓	✓	$\times$	✓
Inversion (exchanges sublattices)	✓	✓	$\times$	$\times$
Time-reversal (reverses spin & $\mathbf{k}$)	✓	✓	✓	✓
Chiral (protects gaplessness)	✓	$\times$	$\times$	$\times$
Charge conjugation ($e^- \leftrightarrow h^+$)	$\times$	$\times$	$\times$	$\times$

Table 1: Symmetries of the Kane-Mele model under the four basic couplings. An ✓ indicates a preserved symmetry, while a $\times$ means it is broken.

$\mathcal{I} = I \otimes \sigma^x$. Notice that in our choice of the gamma matrices $\Gamma^1 = \mathcal{I}$. The condition for a Bloch Hamiltonian to be inversion symmetric is similarly given by (4). If one performs a similar analysis with the gamma matrices as before, one can notice that $\mathcal{I}\Gamma^1\mathcal{I}^{-1} = \Gamma^1$ and $\mathcal{I}\Gamma^{1b}\mathcal{I}^{-1} = -\Gamma^{1b}$, which is in agreement with TR symmetry, but the rest transform in the opposite way under the two symmetries and so must vanish. One can obtain a non-trivial $\mathbb{Z}_2$ topological insulator with both symmetries present, and requiring both symmetries makes the analysis theoretically simpler (this is the path taken, for example, in [9]), but here we will always allow inversion-breaking terms.

Let us now present the specific form the coefficients take in full Kane-Mele model of graphene with the notation $x := \frac{k_x a}{2}$ and $y := \frac{\sqrt{3}}{2} k_y a$ already used in Subsection 3.3:

$$\begin{aligned} d_1 &= t(1 + 2\cos x \cos y) & d_{12} &= -2t \cos x \sin y \\ d_2 &= \lambda_v & d_{15} &= 2\lambda_{so}(\sin(2x) - 2\sin x \cos y) \\ d_3 &= \lambda_R(1 - \cos x \cos y) & d_{23} &= -\lambda_R \cos x \sin y \\ d_4 &= -\sqrt{3}\lambda_R \sin x \sin y & d_{24} &= \sqrt{3}\lambda_R \sin x \cos y \end{aligned} \tag{16}$$

One can then notice that as $\Gamma^{12} = -I \otimes \sigma^y$ and $\Gamma^{15} = \sigma^z \otimes \sigma^y$ the full Hamiltonian can be written as

$$H_{KM}(\mathbf{k}) = \begin{pmatrix} H_H^{\uparrow}(\mathbf{k}) & 0 \\ 0 & H_H^{\downarrow}(\mathbf{k}) \end{pmatrix} + H_R(\mathbf{k})\,, \tag{17}$$

where $H_H^{\uparrow}(\mathbf{k})$ and $H_H^{\downarrow}(\mathbf{k})$ are Haldane Hamiltonians of the form (1) with coefficients (10) with $t_2 = \lambda_{so}$ and $\phi = \pm\frac{\pi}{2}$ respectively. As $\Gamma^{23} = -\sigma^x \otimes \sigma^x$ and $\Gamma^{24} = -\sigma^y \otimes \sigma^x$, the Rashba interaction term reads

$$H_R = d_3(\mathbf{k})\,\sigma^x \otimes \sigma^y - d_{24}(\mathbf{k})\,\sigma^y \otimes \sigma^x + d_4(\mathbf{k})\,\sigma^y \otimes \sigma^y - d_{23}(\mathbf{k})\,\sigma^x \otimes \sigma^x\,.$$

One can notice that it is off diagonal in the spin degrees of freedom (in the first entry of the tensor product appear σ^x and σ^y) and thus it breaks the conservation of the z component of the spin as indicated in Table 1. It also prevents us from viewing the Kane-Mele model just as two Haldane's models which is possible when $\lambda_R = 0$ as can be seen from (17). This is why we assume in the next subsection the absence of the Rashba term.

For topological purposes it is again enough to look just at the effective theory near the K points. We have already obtained it for the term corresponding to λ_{so} in the

equation (12). Now we can write it as

$$H_{so}^{\text{eff}} = \pm\Delta_{so}\,\sigma^z \otimes \sigma^z \qquad \text{with} \qquad \Delta_{so} := 3\sqrt{3}\lambda_{so}\,.$$

This is manifestly TR invariant since under TR the K point exchange which cancels the sign change coming form the spin degrees of freedom. For the Rashba term one has:

$$H_R^{\text{eff}}(\mathbf{k}) = \Delta_R\,(\pm\sigma^y \otimes \sigma^x - \sigma^x \otimes \sigma^y) \qquad \text{with} \qquad \Delta_R := \frac{3}{2}\lambda_R\,, \tag{18}$$

where we neglected also terms linear in $\mathbf{q}$ since we assume $\lambda_R \ll t$ [1].

As these terms couple also the spin degrees of freedom (unlike terms 1, 2 and 12) these are call the spin orbit coupling terms. Their presence can be roughly argued also based on the microscopic physics as has been done for example in [1] but mainly from the point of view of an effective theory presence is justified as they satisfy all the required symmetries (mainly the TR symmetry). There is also a simple physical intuitive picture one can draw which can be well seen in the form of (18). Let us have an electron moving in an electric field $\vec{E}$ with a velocity $\frac{\vec{p}}{m}$, then in the inertial frame of the electron one has magnetic field proportional to $\vec{p}\times\vec{E}$. As the electron has its magnetic moment due to spin $\vec{S}$ the corresponding potential energy will be proportional to $\left(\vec{p}\times\vec{E}\right)\cdot\vec{S} = \left(\vec{S}\times\vec{p}\right)\cdot\vec{E}$ thus if the electric field is in the z direction transverse to the graphene plane one has a potential $\lambda\left(\vec{S}\times\vec{p}\right)\cdot\vec{z}$ where $\vec{z}$ is a unit vector which is a classical equivalent of (18).

Let us now turn to the topology. The case of vanishing λ_R is discussed right in the next section. Ignoring for a second for simplicity the staggered potential term λ_v (can be easily included) the energy gap is for $0 < \Delta_R < \Delta_{so}$ at the K points just $\Delta = 2(\Delta_{so} - \Delta_R)$. Region of such parameters is adiabatically connected to the case of $\lambda_R = 0$. However, if the Rashba term would become too strong so that $\Delta_R > \Delta_{so}$ the gap would close, and we would have electronic structure that of a zero gap semiconductor [1].

4.2 Spin Hall conductivity

Without spin interaction we would have full freedom to choose basis of each fibre of our Bloch bundle which would correspond to $U(2)$ gauge symmetry. This symmetry basically consists of the $U(1)$ phase symmetry we considered in the last section global part of which is at the many-body level responsible for charge conservation and $SU(2)$ symmetry global part of which is responsible for spin conservation. The intrinsic spin orbit interaction breaks the $SU(2)$ symmetry as indicated in Table 1, but it leaves us with another $U(1)$ symmetry which is responsible for conservation of the z component of the spin. We are thus left with a $U(1)\times U(1)$ gauge theory which corresponds to choosing a phase associated to each spin projection. Notice that it is important that the Rashba interaction is absent since that would break also the remaining spin $U(1)$ symmetry and as noted before our discussion assumes that $\lambda_R = 0$.

The total curvature of the $U(1)\times U(1)$ group decomposes as $\rightarrow F(\mathbf{k}) = F_\uparrow(\mathbf{k}) + F_\downarrow(\mathbf{k})$. Using the same argument as in the Subsection 3.2 one can prove that the total Chern number c_1 vanishes due to the presence of TR symmetry. That means

$$0 = c_1 = \frac{1}{2\pi}\int_{\mathbb{T}^2} F = \frac{1}{2\pi}\int_{\mathbb{T}^2} F_\uparrow + \frac{1}{2\pi}\int_{\mathbb{T}^2} F_\downarrow = c_1^\uparrow + c_1^\downarrow \implies c_1^\uparrow = -c_1^\downarrow$$

and this is indeed true in our model. One can readily verify this as $c_1^\uparrow$ is calculated from the Hamiltonian $H_H^\uparrow(\mathbf{k})$ which has $\phi = \pi/2$ and $H_H^\downarrow(\mathbf{k})$ with $\phi = -\pi/2$ and looking at

the phase diagram in the Figure 4 one can see if $|\lambda_v| < 3\sqrt{3}|\lambda_{so}|$ then $c_1^{\uparrow} = 1 = -c_1^{\downarrow}$ and if $|\lambda_v| > 3\sqrt{3}|\lambda_{so}|$ then $c_1^{\uparrow} = 0 = -c_1^{\downarrow}$. However, $c_1^{\uparrow} = -c_1^{\downarrow}$ holds even in models with higher band where is general $c_1^{\uparrow}, c_1^{\downarrow} \in \mathbb{Z}$.

This means that $n_s = \frac{c_1^{\uparrow} - c_1^{\downarrow}}{2} = c_1^{\uparrow} \in \mathbb{Z}$ can be non-vanishing. One can then define spin Hall conductivity naturally a $\sigma_{xy}^s := \frac{\hbar}{e}\frac{\sigma_{xy}^{\uparrow} - \sigma_{xy}^{\downarrow}}{2}$, and then it follows from the TKNN formula (8) that

$$\sigma_{xy}^s = \frac{e}{2\pi} n_\sigma \, .$$

And we see thus see that σ_{xy}^s is quantized, and we have the so-called *quantum spin Hall (QSH) effect*.

Furthermore, from n_s one can define the topological (in the sense of Subsection 2.3) invariant $z_2 \equiv n_s \pmod 2$ which is the celebrated $\mathbb{Z}_2$ invariant. This is probably the most intuitive expression for the $\mathbb{Z}_2$ invariant one can find, but we have to remember that this works just with the simplifying assumption of $\lambda_R = 0$. We will encounter more general expression in Subsection 5.2. We can see that in the region $|\lambda_v| < 3\sqrt{3}|\lambda_{so}|$ our simple model has $z_2 = 1$ as corresponds thus to a non-trivial insulator and in the region $|\lambda_v| < 3\sqrt{3}|\lambda_{so}|$ we have $z_2 = 0$ and a trivial insulator. Furthermore, we see that in this model the region where we have non-trivial spin hall current exactly coincides with a non-trivial insulator.

5 $\mathbb{Z}_2$ topological phase of graphene

In this section we discuss the presence of the edge states and some of their properties. These are certainly of a high interest. Due to their interesting properties, some of which we discuss, they are probably what is most interesting on topological insulators for applications. In this section we allow the presence of the Rashba interaction and extend thus our discussion of the previous section (where it was neglected) to a more realistic setting. At the end we provide an expression of the $\mathbb{Z}_2$ topological invariant in this general setting.

5.1 Helical edge states

One way to argue for the presence of edge states in the Kane-Mele model is based on the Laughlin's argument, which is the way they take in the papers [1, 2], but since we already established their presence of chiral edge states in Haldane's model in the analysis of Subsection 3.4 we are going to make use of that instead.

In the absence of spin-mixing, the Kane-Mele Hamiltonian (17) decomposes into two independent Haldane models with equal and opposite Chern numbers, corresponding to the two spin projections. This means if the system is to be TR invariant, the transition to a trivial insulator must occur simultaneously for both spin sectors. By essentially repeating the argument of Subsection 3.4 for each spin block, we could find that the edge state solutions would again take the form (15), now with an additional spin degree of freedom (and we would have two solution for each spin projection instead of just one). In this case, however, the edge states are not chiral in the strict sense, since there is no single direction in which all states move. Instead, we have the so-called *helical edge states*: the spin is locked to the direction of motion, with spin-up propagating in one direction and spin-down in the opposite direction along the edge. This spin-momentum locking is a defining feature of the general non-trivial $\mathbb{Z}_2$ insulating phase.

As we will see a key property of these helical edge states, as in the chiral case, is the absence of elastic backscattering for non-magnetic disorder: a right-mover cannot scatter into a left-mover without flipping its spin, which is forbidden by TR symmetry. As a result, these edge states are robust and cannot be localized by any TR symmetric perturbation.

Crucially, the gapless edge states persist even when spin-mixing terms, such as the Rashba coupling, are present. In this regime, projection of spin onto the z axis is no longer a good quantum number, so the edge states are not simply spin-up or spin-down. Nevertheless, the general property of spin-momentum locking (helicity) survives, that is each direction of motion along the edge remains associated with a distinct spin state, even if the spin axis is not fixed. This can be demonstrated by solving the model in a geometry infinite in the x direction, as illustrated in Figure 5, which shows the energy spectrum of a strip with two edges in both the non-trivial and trivial insulating phases. In the phase of non-trivial topology, the edge states traverse the bulk gap and cross at $k_x = \pi/a$, while in the trivial insulator the edge states do not cross the gap.

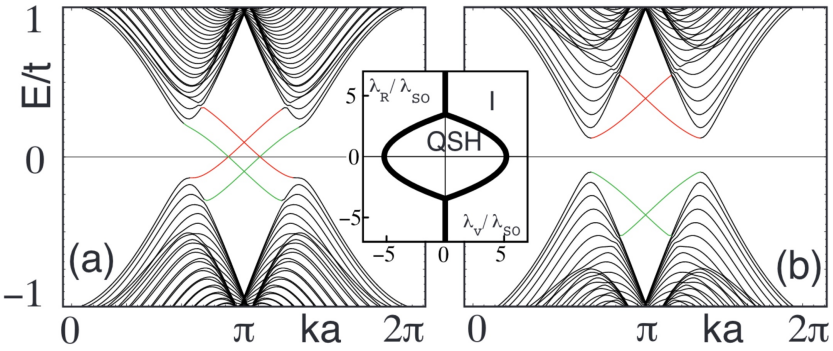

Figure 5: Energy spectrum for a graphene strip with zigzag edges, infinite in the x direction, in (a) the non-trivial $\mathbb{Z}_2$ insulating phase (labelled 'QSH' in the figure) with $\lambda_v = 0.1t$, and (b) the trivial insulating phase with $\lambda_v = 0.4t$. In both cases, $\lambda_{so} = 0.06t$ and $\lambda_R = 0.05t$. The edge states on each edge are shown in different colours and cross at $ka = \pi$ in the non-trivial phase, traversing the bulk gap, while in the trivial insulator the edge states do not cross the gap. The inset shows the phase diagram as a function of λ_v and λ_R for $0 < \lambda_{\rm SO} \ll t$. Adapted from [2].

In a more general case than that in the Subsection 4.2 one may define a spin Hall conductance as rate of spin accumulation per applied perpendicular electric E field, that is by $\frac{d\langle S_z\rangle}{dt} = G^s_{xy}E$, which is then given by

$$G^s_{xy} = \frac{e}{h}\left(\langle S_z\rangle_L - \langle S_z\rangle_R\right)\Big|_{E_F} ,$$

where expectation value of S_z is evaluated for the left and right moving states at the Fermi level. In the absence of spin-mixing, the quantized value obtained in the bulk calculation is confirmed by the edge state analysis, reflecting the robust edge transport. However, once spin-mixing is introduced, the edge states are not eigenstates of S_z, so the spin Hall conductance G^s_{xy} is generally not quantized, though it remains non-zero in the topological phase. Thus, we see that we may detect non-trivial topology by non-zero spin accumulation at the edges, while in the trivial insulator, where edge states are localized by disorder, the spin accumulation vanishes.

The robustness of the helical edge states can be captured elegantly using the S-matrix formalism. Consider a segment of the edge with disorder, and denote by ψ_{in} and ψ_{out} the incoming and outgoing two-component spinors, consisting of the left- and right-moving edge states. Scattering is described by a unitary S-matrix, $\psi_{\text{out}} = S\psi_{\text{in}}$. As we have seen in Subsection 4.1 the TR symmetry is represented on the spin degrees of freedom by $\Theta = i\sigma^y \mathcal{K}$. If we require the scattering process to be TR invariant we must have $[\Theta, S] = 0$. This then imposes in the S-matrix the constraint $S = \sigma_y S^T \sigma_y$, which forces the off-diagonal (backscattering) elements to vanish. As a consequence, an electron propagates perfectly through a region of disorder as long as time-reversal symmetry is preserved and the bulk gap remains open. This ensures that the edge states in the topological $\mathbb{Z}_2$ insulating phase cannot be localized by elastic backscattering, in contrast to ordinary one-dimensional conductors.

However, it is important to note that the presence of gapless edge states alone does not guarantee topological protection. For instance, in certain cases with an even number of Kramers pairs of edge states at a given energy, elastic backscattering is allowed between pairs, and the edge states can be localized by disorder, these are sometimes called 'trivial' metallic edge states. Let us make this distinction more precise. Only an odd number of Kramers pairs intersecting the Fermi level at a given edge signals a truly topologically non-trivial phase. This is illustrated in Fig. 5, where in the topological phase (a) each edge hosts a single Kramers pair crossing the gap, while in the trivial phase (b) the number of crossings is even or zero, and the edge states are not protected. The $\mathbb{Z}_2$ topological invariant therefore counts the parity of Kramers pairs of edge states crossing the Fermi level.

Finally, while the helical edge states are protected against elastic backscattering, inelastic processes arising from electron-electron interactions can still occur, allowing backscattering at finite temperature. These processes do not open a gap or cause localization in the weak-interaction regime, but they do lead to a finite conductivity at non-zero temperatures, distinguishing the $\mathbb{Z}_2$ topological edge from a truly ballistic one-dimensional channel.

5.2 $\mathbb{Z}_2$ topological invariant

As discussed previously, TR symmetry imposes strong constraints on the topology of the valence bundle. In Subsection 3.2, we have seen that in a TR symmetric system the Chern number always vanishes. It is even true that one can always globally and continuously find a basis of the valence bundle $(|u_1(\mathbf{k})\rangle, |u_2(\mathbf{k})\rangle)$, which means, according to the theorem at the end of Subsection 2.1, that the valence bundle is always trivial as a complex vector bundle. However, when we require this basis to consist of Kramers pairs, that is $\Theta |u_1(\mathbf{k})\rangle = |u_2(-\mathbf{k})\rangle$, with Θ being the TR operator introduced in Subsection 4.1, the situation changes. The additional quaternionic structure (as introduced in Subsection 2.3) allows for a more subtle topological obstruction, captured by the $\mathbb{Z}_2$ invariant.

A key role is played by the overlap matrix

$$\mathbb{P}_{ij}(\mathbf{k}) = \langle u_i(\mathbf{k})| \, \Theta \, |u_j(\mathbf{k})\rangle \ ,$$

[5] which is always antisymmetric by construction (from $\Theta^2 = -I$). For antisymmetric matrices, the determinant turns out to be the square of a polynomial in the matrix

[5] This again has the inconvenience of taking products of states at different fibres, which is why the 'sewing matrix' is sometimes used instead (see for example [9]).

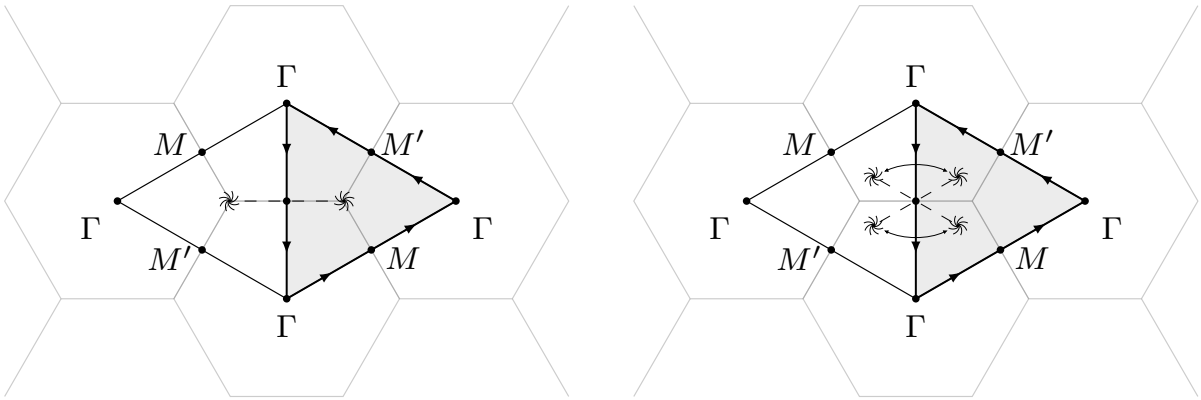

(a) Non-trivial case

(b) Trivial case

Figure 6: Illustration of the Pfaffian vortices in the graphene Brillouin zone (rhombus). Shaded is a domain U chosen according to TR symmetry and the TRIM points are represented by black dots. The spiral symbols denote vortices (zeros) of the Pfaffian $P(\mathbf{k})$, with the direction of the spirals indicating vorticity. Dashed lines connect each pair of TR related vortices of opposite vorticity.

entries. This motivates introducing the Pfaffian of an antisymmetric matrix $\mathbb{A}$, defined so that $\mathrm{Pf}(\mathbb{A})^2 = \det \mathbb{A}$. With this, we define

$$P(\mathbf{k}) = \mathrm{Pf}[\mathbb{P}(\mathbf{k})]\,.$$

In the case of two occupied bands, $\mathbb{P}(\mathbf{k})$ is just a 2×2 antisymmetric matrix, so the Pfaffian just picks out the single independent entry, but it is handy for generalizing to higher dimensions.

The zeros of the Pfaffian are of particular importance: at a point $\mathbf{k}_*$ where $P(\mathbf{k}) = 0$, the valence band and its TR partner become orthogonal, which indicates an obstruction to the definition of a global Kramers basis (this is shown for the case with inversion symmetry in [9]). The presence of such zeros, in the following referred to as 'vortices', can be intuitively thought of as giving the quaternionic vector bundle a twist, inducing a non-trivial topology. They are depicted in Figure 6 by small vortices. Calling the complex zeros vortices makes sense, as one can assign to them an order (which we will call vorticity) by calculating the winding number of $P(\mathbf{k})$. Because of the TR symmetry, in the Brillouin zone these zeros always come in TR pairs at $\mathbf{k}_*$ and $-\mathbf{k}_*$, always with vorticities $+1$ and -1. The pairing of the vortices is indicated in Figure 6 by the dotted lines connecting the pair members.

A crucial property emerges at the time-reversal invariant momenta (TRIM) introduced in Subsection 4.1. At a TRIM point $\boldsymbol{\lambda}$, the action of time reversal on the basis $(|u_1(\boldsymbol{\lambda})\rangle\,, |u_2(\boldsymbol{\lambda})\rangle)$ yields another basis at the same point. Specifically, the transformation can be written as $\Theta\,|u_i(\boldsymbol{\lambda})\rangle = \mathbb{U}_{ij}\,|u_j(\boldsymbol{\lambda})\rangle$ for some 2×2 antisymmetric unitary matrix $\mathbb{U}$ ($\mathbb{U}\mathbb{U}^\dagger = I$ and $\mathbb{U}^T = -\mathbb{U}$). This property ensures that the absolute value of the Pfaffian at these points is always unity as $|P(\boldsymbol{\lambda})| = |\,\mathrm{Pf}(\mathbb{U})| = \sqrt{|\det \mathbb{U}|} = 1$. Thus, vortices of the Pfaffian can never occur at TRIM points.

The two properties of the zeros of $P(\mathbf{k})$, that they come in pairs of opposite vorticity and cannot cross the TRIM points, imply that the relevant topological information is encoded in the number of vortex pairs modulo 2. Since the vortices represent a fundamental obstruction to globally defining Kramers pairs, the insulator is trivial if and only if all vortices can be eliminated by adiabatic transformations. As indicated in Subfigure 6a, two

pairs of vortices can be mutually annihilated by adiabatically moving vortices of opposite vorticity to the same point. The case of a single vortex pair is shown in Subfigure 6b; in this situation, the vortices cannot be annihilated, as this would require passing through a TRIM point, which is forbidden since vortices cannot enter TRIM points.

To quantify the parity of the number of vortex pairs, we introduce the following integral expression. Since TR symmetry introduces a redundancy in the description, we cover the Brillouin torus with a region U (shown in grey in Figure 6) and its image under the map $\theta(\mathbf{k}) = -\mathbf{k}$, so that $U \cup \theta(U) = \mathbb{T}^2$. It is important to choose U so that the zeros of the Pfaffian do not lie on the boundary ∂U. The winding number of the phase of the Pfaffian along this boundary,

$$z_2 = \frac{1}{2\pi i} \oint_{\partial U} d \log P(\mathbf{k}) \mod 2 \,,$$

gives precisely the desired parity of the number of vortex pairs, and we declare this to be the $\mathbb{Z}_2$ invariant. $z_2 = 1$ indicates a non-trivial topology, and $z_2 = 0$ a trivial insulator. This construction bears a clear analogy to the approach in Subsection 3.2, where the Chern topological invariant was expressed as a contour integral of a transition function over the boundary between regions of different gauges. In this way, the $\mathbb{Z}_2$ invariant robustly distinguishes topological insulators from trivial ones in the presence of TR symmetry, even when the Hamiltonian includes spin-mixing terms such as the Rashba coupling.

Bibliography

[1] C. L. Kane and E. J. Mele. Quantum Spin Hall Effect in Graphene. *Physical Review Letters*, 95(22):226801, November 2005. doi:10.1103/PhysRevLett.95.226801. Publisher: American Physical Society.

[2] C. L. Kane and E. J. Mele. $\mathbb{Z}_2$ Topological Order and the Quantum Spin Hall Effect. *Physical Review Letters*, 95(14):146802, September 2005. doi:10.1103/PhysRevLett.95.146802.

[3] K. V. Klitzing, G. Dorda, and M. Pepper. New Method for High-Accuracy Determination of the Fine-Structure Constant Based on Quantized Hall Resistance. *Physical Review Letters*, 45(6):494–497, August 1980. ISSN 0031-9007. doi:10.1103/PhysRevLett.45.494.

[4] D. J. Thouless, M. Kohmoto, M. P. Nightingale, and M. Den Nijs. Quantized Hall Conductance in a Two-Dimensional Periodic Potential. *Physical Review Letters*, 49 (6):405–408, August 1982. ISSN 0031-9007. doi:10.1103/PhysRevLett.49.405.

[5] F. D. M. Haldane. Model for a Quantum Hall Effect without Landau Levels: Condensed-Matter Realization of the "Parity Anomaly". *Physical Review Letters*, 61 (18):2015–2018, October 1988. ISSN 0031-9007. doi:10.1103/PhysRevLett.61.2015.

[6] M. König, S. Wiedmann, C. Brüne, A. Roth, H. Buhmann, L. W. Molenkamp, X.-L. Qi, and S.-C. Zhang. Quantum Spin Hall Insulator State in HgTe Quantum Wells. *Science*, November 2007. doi:10.1126/science.1148047.

[7] A. Kitaev. Periodic table for topological insulators and superconductors. In *AIP Conference Proceedings*, pages 22–30, 2009. doi:10.1063/1.3149495.

[8] M. Aghaee, A. Alcaraz Ramirez, Z. Alam, et al. Interferometric single-shot parity measurement in InAs–Al hybrid devices. *Nature*, 638(8051), February 2025. ISSN 1476-4687. doi:10.1038/s41586-024-08445-2.

[9] M. Fruchart and D. Carpentier. An introduction to topological insulators. *Comptes Rendus Physique*, 14(9):779–815, November 2013. ISSN 1631-0705. doi:10.1016/j.crhy.2013.09.013.

[10] S. van Nigtevecht. Topological phases and K-theory, 2019. URL: `https://webspace.science.uu.nl/~0554804/publications/bachelor.pdf`. Bachelor's thesis, Utrecht University.

[11] D. S. Freed and G. W. Moore. Twisted Equivariant Matter. *Annales Henri Poincaré*, 14(8):1927–2023, December 2013. ISSN 1424-0661. doi:10.1007/s00023-013-0236-x.

[12] C. L. Kane. Topological Band Theory and the $\mathbb{Z}_2$ Invariant. In M. Franz and L. Molenkamp, editors, *Contemporary Concepts of Condensed Matter Science*, volume 6 of *Topological Insulators*, pages 3–34. Elsevier, January 2013. doi:10.1016/B978-0-444-63314-9.00001-9.

[13] J. L. Dupont. Symplectic Bundles and KR-Theory. *MATHEMATICA SCANDINAVICA*, 24:27–30, December 1969. ISSN 1903-1807. doi:10.7146/math.scand.a-10918.